

Using computational fluid dynamics to predict the erosion rates on the cyclones wall for coal boiler plant

B. Anindito, T. Nurtono and S. Winardi

Department of Chemical Engineering, Institut Teknologi Sepuluh Nopember, Surabaya, Indonesia
Phone: +62315999282; Fax: +62315999282

ABSTRACT – In the industrial coal boiler, cyclone is used to separate the silica sands (as fluidizing medium) from the furnace combustion gas. A gas-solid separation system with turbulent swirling flow that occurs in the cyclone will cause erosion on the cyclone wall. The erosion will cause a decrease in the cyclone performance and increase the maintenance cost. CFD simulation was conducted to predict this erosion using industrial cyclone in the coal boiler industry on its actual dimensions. The dimensions were 5120 mm in diameter and 13970 mm in height. It was performed using the Reynolds Stress Model (RSM) for turbulence flow in the gas phase and the Oka erosion model. The erosion rate on the cyclone wall was investigated at various gas inlet velocity and solid rate. The inlet velocities ranged from 6 to 8 m/s and the solid rates ranged from 30 to 40 kg/s with silica sands as solid particles (0.075 and 1.5 mm in diameter). At the selected local area, the results showed that the higher gas inlet velocity for the same solid rate would increase the erosion rate (about 25%). However, the higher solid rate for the same velocity will also increase the erosion rate on the cyclone wall (about 18%). These results indicate that cyclone wall erosion are significantly affected by inlet gas velocity.

ARTICLE HISTORY

Received: 11th Oct 2019

Revised: 30th Sept 2020

Accepted: 26th Oct 2020

KEYWORDS

*Computational fluid dynamics;
erosion rate;
cyclone;
coal boiler*

INTRODUCTION

Gas-solid separation is a general process which often used in industry. Various types of equipment have been commonly used for gas-solid separation such as cyclone separator, bag filter and electrostatic precipitators [1, 2]. Cyclone separator is the most commonly used in industries due to its several advantages compared with other equipment, such as low installation, operational and maintenance costs, no moving components (static parts). Moreover, and it has an ability to operate at high temperature up to 1000 °C, high pressure up to 100 bar and a high rate of solid particles [3-8]. The main parts of cyclone separator consist of a cylindrical section, conical section, tangential inlet, clean gas outlet (called vortex finder), solid particle outlet and solid particle collector or bin. The basic principle of cyclone was the gas stream contains solid particles entering the inlet section tangentially with high angular velocity and formed swirling flow [9, 10]. The disperse solid particles in the gas flow are forced in the radial outward to the wall by centrifugal force and move down along the cyclone wall into the solid particle collector or bin. The gas swirls upwards in the centre of the cyclone and leaves the cyclone through a vortex finder [8, 11, 12]. The main problem that often occurs in cyclone separator is wall erosion. This is due to the interaction of solid particles with the cyclone wall which further affects the operational and financial consequences. Before modelling the erosion rate on the wall of the cyclone, the gas-solid hydrodynamic flow must be known at first. Even though the design and geometric construction of cyclone separator are quite simple but the phenomena are quite complex. The swirling flow inside the cyclone separator has strong anisotropy flow, high turbulence flow, and high gas-solid wall friction [13].

A numerical method such as CFD has been commonly used to carry out some simulation process [14-16]. Several previous studies have been carried out to investigate the hydrodynamic flow and erosion rates both experimental and simulation which mostly carried out on small scale cyclones. Masnadi et al. [17] investigated the distribution of gas-solid multiphase flow and the effect of cyclone geometry on its performance [18, 19]. Cyclone geometry is the main factor affecting its performance (pressure drop and separation efficiency) [20-22]. These studies utilize CFD simulation code using the Eulerian-Lagrangian approach (Reynolds turbulence model) for continuous gas flow and discrete phase model (DPM) for dispersed particles [23, 24].

Research on erosion in elbow piping systems due to the flow of sand particles using the CFD code was carried out by Parsi et al. [25] through the Lagrangian approach using 4 different types of erosion equation model which are Oka, DNV (Det Norske Veritas), Zhang and Mansouri's models with a One-Way coupling. Sedrez et al. [26] are using the Eulerian-Lagrangian approach with the Reynolds Stress Model (RSM) with two-way coupling and 2 types of erosion modelling which are DNV and Oka. In addition, Sedrez also carried out an experiment for the CFD code validation. Based on the simulation results and experimental validation, erosion rate increases as the gas velocity increases and the rate of erosion

rate decreases as the ratio of solids increases. However, none of these studies using the real geometry same as used in the industrial process.

In this study, therefore, CFD code was used to investigate the erosion rate of the cyclone separator using actual geometry as used in the industry. The input operational condition data such as velocity and mass solid rate were obtained from an industrial scale coal boiler plant.

METHODS AND MATERIALS

The Geometry of the Cyclone Separator

The material of the cyclone separator made from carbon steel in the outer part, while the inner part made from castable refractory. The Geometry and dimension of the cyclone were shown in Figure 1 and Table 1, respectively.

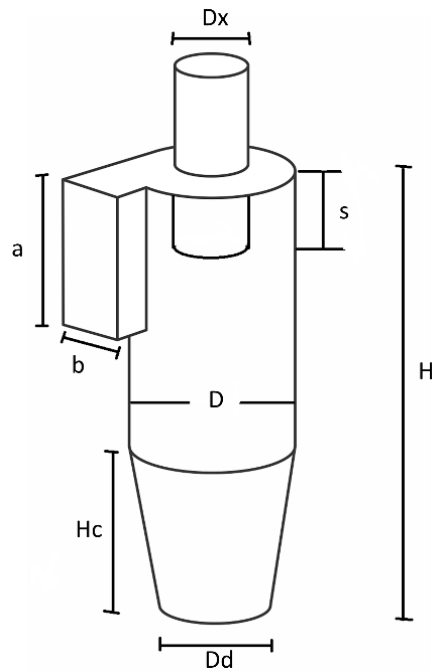


Figure 1. The geometry of cyclone separator

Table 1. The dimension of cyclone separator

Dimension	Size (mm)
Cyclone diameter (D)	5,120
Cyclone height (H)	13,970
Diameter of vortex finder (Dx)	2,200
Length of vortex finder (s)	2,310
Tangential inlet height (a)	4,620
Tangential inlet width (b)	2,333
Conical cyclone height (Hc)	5,200
Dust exit diameter (Dd)	3,320

Data and Validation Method

As mentioned before, the data used in the CFD simulation is the actual data from the coal boiler plant. Silica sand samples (as solid particles dispersed in the continuous gas phase) are taken at the inlet of the cyclone separator and the distribution of the particles is shown in Table 2. Samples of part of the cyclone wall were taken to determine their physical properties. In addition, operational conditions data such as inlet velocity and solid mass rate were obtained during the operation of the coal boiler plant at turnaround or shutdown (which is scheduled every six months). All data were used

as input data in CFD simulation. The validation method is done by measuring the depth of erosion along the cyclone wall. The erosion rate was validated only at the 8 m/s for inlet velocity and 40 kg/s for a solid mass rate of the actual operation of coal boiler plant.

Table 2. Solid particle size distribution

Size (micron)	Total weight (%)	Size (micron)	Total weight (%)
2,000	0.14	180	17.10
1,000	0.30	150	8.80
710	0.30	125	6.80
425	7.24	106	4.20
355	8.60	<75	4.92
212	41.60	-	-

CFD Simulation of Cyclone Separator

CFD is a numerical algorithm which can be used to simulate fluid flow, mass transfer, heat transfer or other phenomena using computer simulations [27, 28]. To calculate, analyse and simulate a system, CFD requires data variables, input data, outputs, equations and boundary conditions of the system. In general, a CFD code consists of three elements: pre-processor, solver and post-processor. Hydrodynamic flow and particle tracking were conducted before calculation of the erosion rate. Eulerian approach (with continuity and momentum transport) is used to solve the continuous flow and the time-averaged Navier-Stokes (RANS) equations. Particle trajectory and velocity as a discrete phase predicted using Newton's law motion equations in Lagrangian framework, using two-way coupling with the continuous phase. turbulence modelling was conducted using the Reynolds stress model (RSM) due to its property to predict the strong turbulent swirling flow with anisotropic behaviour [24]. In a turbulent flow, the particle trajectories can be affected by the fluctuations of the velocity. Discrete random walk model (DRW) was used to investigate the turbulence fluctuation velocity components on the particle trajectories [29].

Mathematical Models

The gas-solid flow is simulated using Eulerian equation. Gas as the continuous phase and the solid as the discrete phase. The equation used is as follows:

Lagrangian equation – Discrete phase [30]

$$\frac{dx_p^{(i)}}{dt} = v_p^{(i)} \quad (1)$$

$$\frac{dv_p^{(i)}}{dt} = \left(\frac{\rho_p - \rho_g}{\rho_p} \right) g + \frac{18\mu_g}{\rho_p (d_p^{(i)})^2} \left(\frac{C_D^{(i)} \text{Re}_p^{(i)}}{24} (v_g - v_p^{(i)}) \right) \quad (2)$$

with, $C_D^{(i)} = a_1 + \frac{a_2}{\text{Re}_p^{(i)}} + \frac{a_3}{(\text{Re}_p^{(i)})^2}$; $\text{Re}_p^{(i)} = \frac{\rho_g d_p^{(i)} |v_g - v_p^{(i)}|}{\mu_g}$

Eulerian equation – Continuous Phase [30]

Continuity equation:

$$\frac{\partial}{\partial t} (\rho_g) + \nabla (\rho_g v_g) = 0 \quad (3)$$

Momentum equation:

$$\frac{\partial}{\partial t} (\rho_g v_g) + \nabla (\rho_g v_g v_g) = -\nabla P_g - \nabla (T^V + T^R) + \rho_g g + S_v \quad (4)$$

where the index g represents the gas phase, v is a velocity vector.

The turbulence flow used the RSM model as follows in Eq. (5) [30].

$$\begin{aligned} \frac{\partial}{\partial t}(\overline{T^R}) + \nabla_{v_g}(\overline{T^R}) = & -\rho_g \left| v'_g v'_g \cdot (\nabla_{v_g})^T + (\nabla_{v_g}) v'_g v'_g \right| - \rho_g \varepsilon_g \left[C_{s1} b + C_{s2} \left(b \cdot b - \frac{1}{3} b : b \delta \right) \right] - C_{r1} \Psi \cdot b + \\ & C_{r2} \rho_g k_g S_d - C_{r3} \rho_g k_g S_d \sqrt{b : b} + C_{r4} \rho_g k_g \left(b \cdot S_d^T + S_d \cdot b^T - \frac{2}{3} b : S_d \delta \right) + C_{r5} \rho_g k_g \left(b \cdot \Omega^T + \Omega \cdot b^T \right) + \\ & \nabla \left(\frac{\mu_{t,g}}{\sigma_{k,g}} \nabla v'_g v'_g \right) + \nabla (\mu_g \nabla v'_g v'_g) - \frac{2}{3} \sigma \rho_g \varepsilon_g \end{aligned} \quad (5)$$

where,

$$b = \frac{v'_g v'_g}{k_g} - \frac{2}{3} \delta ; S_d = \frac{1}{2} \left[\nabla_{v_g} + (\nabla_{v_g})^T \right] ; \Omega = \frac{1}{2} \left[\nabla_{v_g} - (\nabla_{v_g})^T \right] ; k_g = \frac{1}{2} v'_g v'_g ; \mu_{t,g} = \rho_g C_\mu \left(\frac{k_g^2}{\varepsilon_g} \right)$$

Erosion Model (Oka Erosion Model) [31]

$$E^{(I)} = 1 \times 10^{-9} E_V \cdot \rho_W \cdot m_p \quad (6)$$

with,

$$E_V = f(\alpha) E_{90} ; E_{90} = L (H_V)^{k1} \left(\frac{v_p^{(i)}}{v'} \right)^{k2} \left(\frac{d_p}{d'} \right)^{k3} ; f(\alpha) = (\sin \alpha)^{n1} (1 + H_V (1 - \sin \alpha))^{n2}$$

where E_V is the volumetric erosion rate ($\text{mm}^3\text{kg}^{-1}$), ρ_W is the density of the wall material, E_{90} is the erosion damage at a normal impact angle ($\text{mm}^3\text{kg}^{-1}$), v' is the reference impact velocity ($\text{m}\cdot\text{s}^{-1}$), d_p is the particle diameter (m), d' is the reference particle diameter (m), H_V and is the material Vickers hardness (GPa).

RESULTS AND DISCUSSION

Cyclone swirl flow requires a moment of inertia which means that it is strongly influenced by the size of the solid particle, solid rate and inlet velocity. The drag force on the smaller particles is larger than the centrifugal force preventing their movement to the cyclone wall. Therefore, the small particles escape downwards in a spiral pattern and the larger particles are collected at the walls [27]. Figure 2 shows the solid particle distribution at the main body of the cyclone. It can be seen at higher inlet velocity, increasing the moment inertia of solid particles in the cyclone resulted in a swirl flow closer to the cyclone wall. The erosion on the cyclone wall will increase due to there is higher friction between the solid particles with the cyclone wall. A Similar trend is seen at a higher solid rate. The more particles enter the cyclone, the more collision with the cyclone wall which further increased in erosion rate.

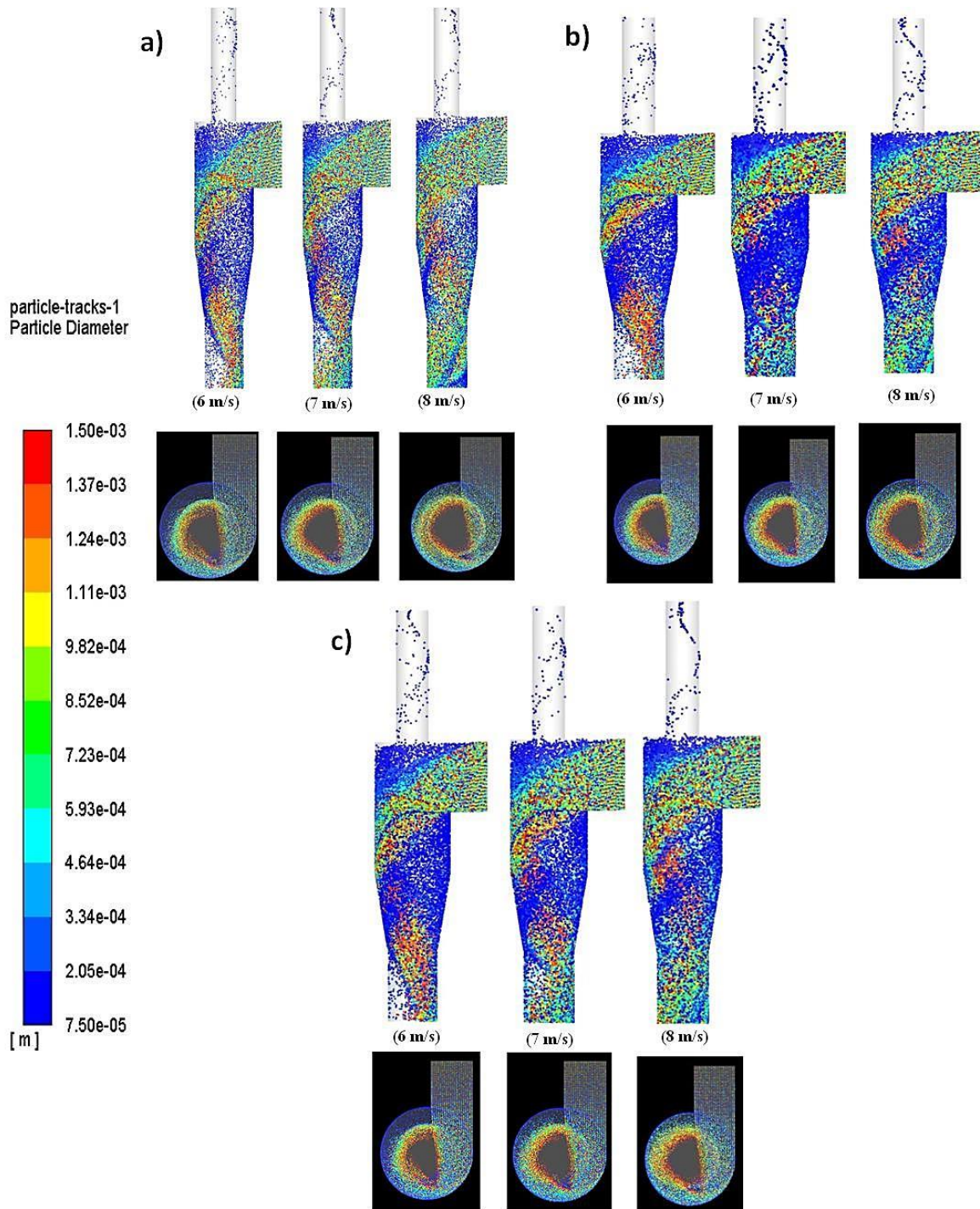


Figure 2. Distribution of solid particles inside cyclone at various inlet velocities from 6 to 8 m/s: (a) solid rate 30 kg/s (b) solid rate 35 kg/s and (c) solid rate 40 kg/s

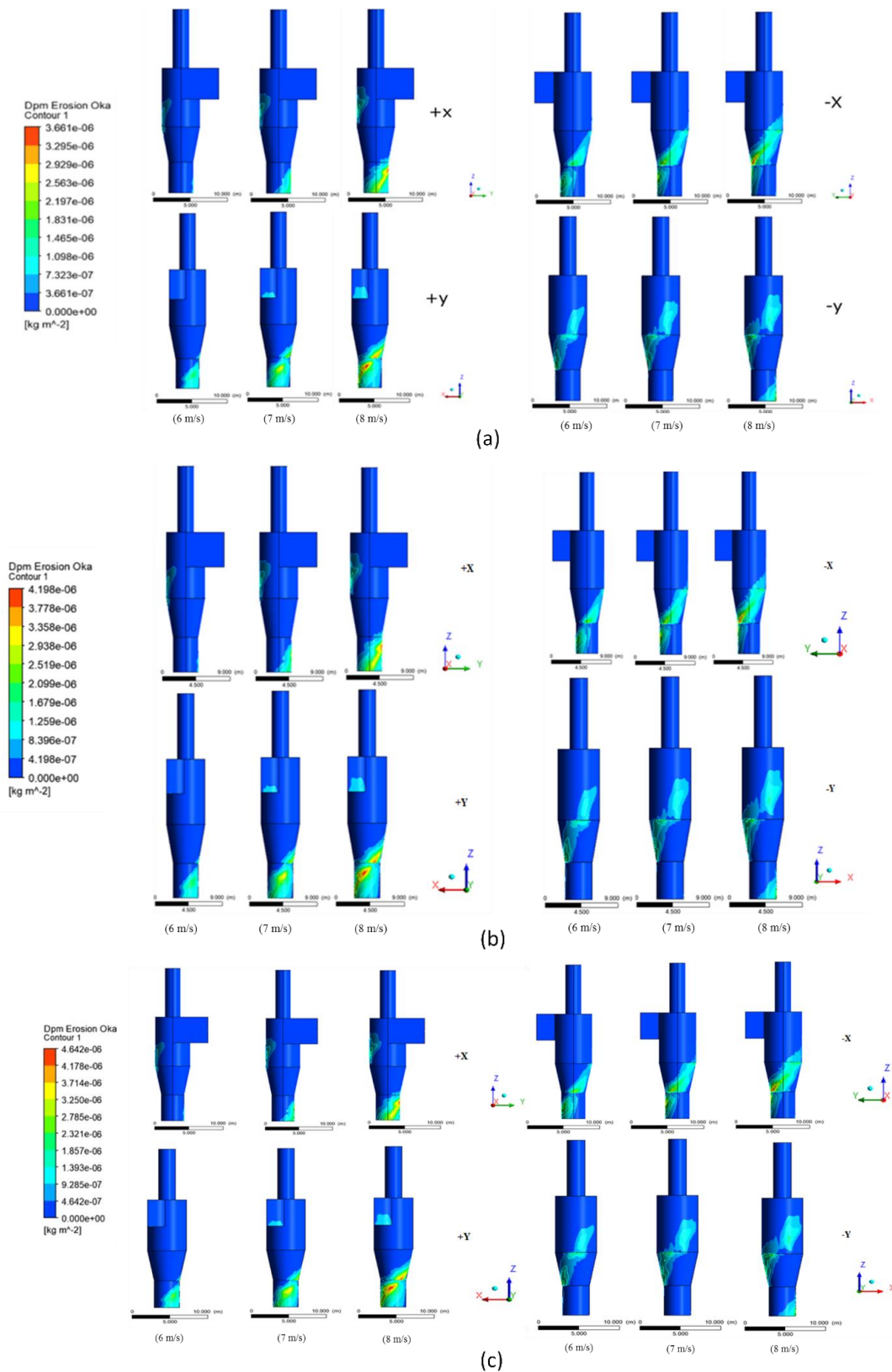


Figure 3. Contour of erosion rate using Oka erosion model at various inlet velocities from 7 to 8 m/s: (a) solid rate 30 kg/s, (b) solid rate 35 kg/s and (c) solid rate 40 kg/s

Erosion rate prediction on the cyclone wall will be calculated using the Oka’s erosion model. Figure 3 shows the erosion contours in the entire cyclone wall To be able to see the erosion contours, the simulation results are shown in 4 directions, which are -X, -Y, + X and + Y. Figure 3 shows that the erosion rate increase with increasing inlet velocities from 7 to 8 m/s and increasing the solid rates from 30 to 40 kg/s. The discussion will focus on the worst erosion in 2 areas, cylindrical section and conical section. The most severe erosion in the cylindrical section area can be seen in the impact zone cylindrical section (-Y direction). The impact zone is an area where initial collisions occur then the direction

of flow changes from tangential flow to angular or swirl flow. Unlike the cylindrical section, for the most severe erosion of the conical section is at the end of the conical section (+Y direction). The highest erosion rate occurs at the inlet velocity 8 m/s and solid rate 40 kg/s, at the cylindrical section of 2.054×10^{-6} kg/m²s and the conical section of 4.538×10^{-6} kg/m²s.

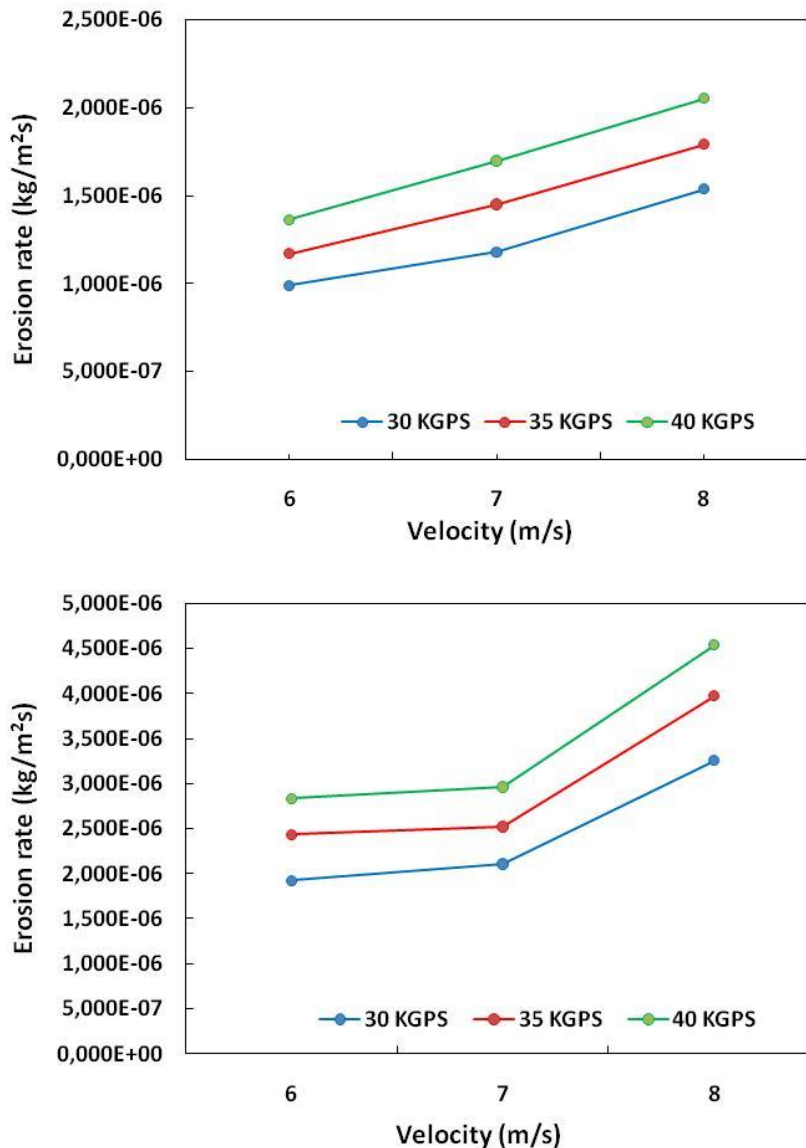


Figure 4. Severe erosion rate with inlet velocities ranged from 7 to 8 m/s and solid rate 30 to 40 kg/s at: (a) cylindrical section and (b) conical section

The comparison of erosion rates for various inlet velocity and solid rate can be seen in Figure 4(a) and (b). Figure 4(a) shows the erosion rate occurs in cylindrical sections while Figure 4(b) in the conical section. The erosion rate increases for the variation of inlet velocity at the cylindrical section by 23.72% and in the conical section by 30.44% at the average. As the solid rate increase, the average erosion rate increases at cylindrical sections by 17.69% and at the conical section by 19.43%. It was mentioned earlier that the validation results were obtained from the actual data on the coal boiler plant. Erosion rate data is based on the erosion of castable wall in the cyclone separator. The cyclone separator operates with fluctuating inlet velocity and solid rate, depending on operational requirements but based on daily data records for 6 months. The average cyclone separator can operate at the inlet velocity 8 m/s and solid rate 40 kg/s. Due to the limitations of validation data, only 1 condition of this variable can be compared between actual data and simulation results. The real condition of the cyclone wall erosion can be seen in Figure 5 and 6. The measurement result showed that the erosion rate on the cyclone wall in cylindrical sections was 2 cm and 4.5 cm for conical sections. These results can be converted into erosion rate units which are 2.05×10^{-6} kg/m².s on the cylindrical section are and 4.54×10^{-6} kg/m².s in the conical section of. Validation data are compared with the simulation results on the same variable, velocity 8 m/s and solid rate 40 kg/s, the percent error is about 23.5% at the cylindrical section and 25.78% in the conical section.



Figure 5. Erosion on cyclone wall at cylindrical section

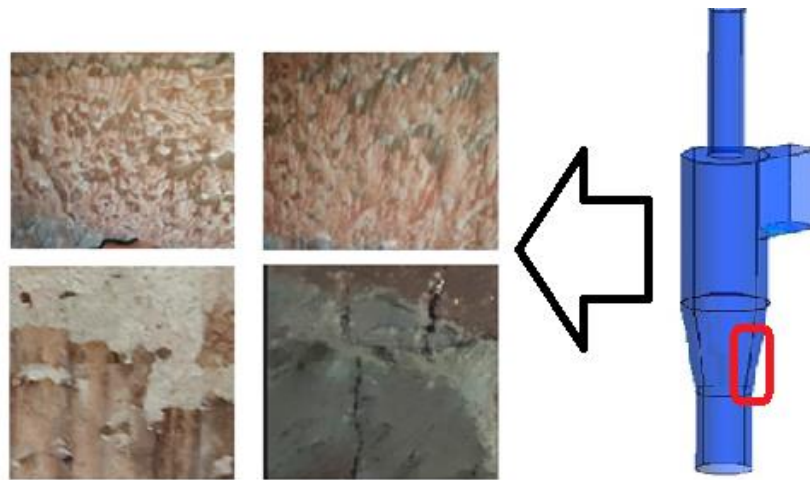


Figure 6. Erosion on cyclone wall at conical section

CONCLUSIONS

In summary, CFD simulation was conducted to predict the erosion rate in the cyclone separator. The inlet velocity and mass solid rate were varied to understand the effect on the wall erosion rate. CFD simulation results show that the inlet velocity has a high dominant impact on the cyclone erosion rate. It caused severe erosion around 30.44% on the conical section. The mass solid rate will be caused erosion of about 19.43% on the conical section. These results show that the inlet velocity variable is more dominantly influencing the cyclone wall erosion. The comparison between simulation results with the real condition, there is still a large error percentage of around 25%. This is caused by many factors that have not been included in the simulation due to data limitations. Several factors that can influence the simulation results include collisions between particles, heat energy in the cyclone system and other factors.

REFERENCES

- [1] Z. Gao, J. Wang, J. Wang, and Y. Mao, "Time-frequency analysis of the vortex in cylindrical cyclone separator," *Chemical Engineering Journal*, vol. 373, pp. 1120-1131, 2019, doi: 10.1016/j.cej.2019.05.054.
- [2] S. Demir, A. Karadeniz, and M. Aksel, "Effects of cylindrical and conical heights on pressure and velocity fields in cyclones," *Powder Technology*, vol. 295, pp. 209-217, July 2016, doi: 10.1016/j.powtec.2016.03.049.
- [3] S. Danyluk, W. J. Shack, and J. Y. Park, "The erosion of a type 310 stainless steel cyclone from a coal gasification pilot plant," *Wear*, vol. 63, pp. 95-104, August 1980, doi: 10.1016/0043-1648(80)90076-9.
- [4] A. Huang, K. Ito, T. Fukasawa, K. Fukui, and H. Kuo, "Effects of particle mass loading on the hydrodynamics and separation efficiency of a cyclone separator," *Journal of the Taiwan Institute of Chemical Engineers*, vol. 90, pp. 61-67, September 2018, doi: 10.1016/j.jtice.2017.12.016.
- [5] P. Liu, Y. Ren, M. Feng, D. Wang, and D. A. Hu, "Performance analysis of inverse two-stage dynamic cyclone separator," *Powder Technology*, vol. 351, pp. 28-37, 1 Juni 2019, doi: 10.1016/j.powtec.2019.04.002.

- [6] S. Y. Noh, J. E. Heo, S. H. Woo, S. J. Kim, M. H. Ock, Y. J. Kim, and S. Yook, "Performance improvement of a cyclone separator using multiple subsidiary cyclones," *Powder Technology*, vol. 338, pp. 145-152, October 2018, doi: 10.1016/j.powtec.2018.07.015.
- [7] D. Misiulia, A. G. Andersson, and T. S. Lundström, "Computational investigation of an industrial cyclone separator with helical-roof inlet," *Chemical Engineering & Technology*, vol. 38, no. 8, pp. 1425-1434, 2015, doi: 10.1002/ceat.201500181.
- [8] S. Wang, H. Li, R. Wang, X. Wang, R. Tian, and Q. Sun, "Effect of the inlet angle on the performance of a cyclone separator using CFD-DEM," *Advanced Powder Technology*, vol. 30, pp. 227-239, February 2018, doi: 10.1016/j.apt.2018.10.027.
- [9] A. C. Hoffman and L. E. Stein, "Gas cyclone and swirl tubes," Springer, Chapter 2, pp. 45-48, 2008.
- [10] M. Jia, D. Wang, C. Yan, J. Song, Q. Han, F. Chen, and Y. Wei, "Analysis of the pressure fluctuation in the flow field of a large-scale cyclone separator," *Powder Technology*, vol. 343, pp. 49-57, 1 February 2018, doi: 10.1016/j.powtec.2018.11.007.
- [11] K. S. Lim, H. S. Kim, and K. W. Lee, "Characteristics of the collection efficiency for a cyclone with different vortex finder shapes," *Journal of Aerosol Science*, vol. 35, pp. 743-754, 2004, doi: 10.1016/j.jaerosci.2003.12.002.
- [12] Y. Li, G. Qin, Z. Xiong, Y. Ji, and L. Fan, "The effect of particle humidity on separation efficiency for an axial cyclone separator," *Advanced Powder Technology*, vol. 30, no. 4, pp. 724-731, April 2019, doi: 10.1016/j.apt.2019.01.002.
- [13] I. Karagoz and A. Avci, "Modelling of the pressure drop in tangential inlet cyclone separators," *Aerosol Science and Technology*, vol. 39, pp. 857-865, 2005, doi: 10.1016/j.jaerosci.2003.12.002.
- [14] S. Hoseinzadeh and P. S. Heyns, "Thermo-structural fatigue and lifetime analysis of a heat exchanger as a feedwater heater in power plant," *Engineering Failure Analysis*, vol. 113, pp. 104548, July 2020, doi: 10.1016/j.engfailanal.2020.104548.
- [15] S. Hoseinzadeh, A. Moafi, A. Shirkani, and A. J. Chamkha, "Numerical validation heat transfer of rectangular cross-section porous fins," *Journal of Thermophysics and Heat Transfer*, vol. 33, 2019, doi: 10.2514/1.T5583.
- [16] S. Hoseinzadeh, R. Ghasemiasl, D. Havaei, and A. J. Chamkha, "Numerical investigation of rectangular thermal energy storage units with multiple phase change materials," *Journal of Molecular Liquids*, vol. 271, pp. 655-660, 1 December 2018, doi: 10.1016/j.molliq.2018.08.128.
- [17] M. S. Masnadi, J. R. Grace, S. Elyasi, and X. Bi, "Distribution of multi-phase gas-solid flow across identical parallel cyclones: Modeling and experimental study," *Separation and Purification Technology*, vol. 72, no. 1, pp. 48-55, 30 March 2010, doi: 10.1016/j.seppur.2009.12.027.
- [18] A. Kepa, "The effect of a counter-cone position on cyclone performance," *Separation Science and Technology*, vol. 47, no. 16, pp. 2250-2255, November 2012, doi: 10.1080/01496395.2012.671878.
- [19] T. C. Hsiao, D. R. Chen, P. S. Greenberg, and K. W. Street, "Effect of geometric configuration on the collection efficiency of axial flow cyclones," *Journal of Aerosol Science*, vol. 42, no. 2, pp. 78-86, February 2011, doi: 10.1016/j.jaerosci.2010.11.004.
- [20] H. Safikhani, "Modeling and multi-objective Pareto optimization of new cyclone separators using CFD, ANNs and NSGA II algorithm," *Advanced Powder Technology*, vol. 27, no. 5, pp. 2277-2284, September 2016, doi: 10.1016/j.apt.2016.08.017.
- [21] M. Wasilewski and L. S. Brar, "Effect of the inlet duct angle on the performance of cyclone separators," *Separation and Purification Technology*, vol. 213, pp. 19-33, 15 April 2019, doi: 10.1016/j.seppur.2018.12.023.
- [22] Q. Wei, G. Sun, and J. Yang, "A model for prediction of maximum-efficiency inlet velocity in a gas-solid cyclone separator," *Chemical Engineering Science*, vol. 204, pp. 287-297, 31 August 2019, doi: 10.1016/j.ces.2019.03.054.
- [23] L. S. Brar, R. P. Sharma, and K. Elsayed, "The effect of the cyclone length on the performance of stairmand high-efficiency cyclone," *Powder Technology*, vol. 286, pp. 668-677, December 2015, doi: 10.1016/j.powtec.2015.09.003.
- [24] A. Sakin, I. Karagoz, and A. Avci, "Performance analysis of axial and reverse flow cyclone separators," *Chemical Engineering and Processing: Process Intensification*, vol. 144, p. 107630, October 2019, doi: 10.1016/j.cep.2019.107630.
- [25] M. Parsi, M. Agrawal, V. Srinivasan, R. E. Vieira, C. F. Torres, B. S. McLaury, and S. A. Shirazi, "CFD simulation of sand particle erosion in gas-dominant multiphase flow," *Journal of Natural Gas Science and Engineering*, vol. 27, no. 2, pp. 706-718, November 2015, doi: 10.1016/j.jngse.2015.09.003.
- [26] T. A. Sedrez, R. K. Decker, M. K. Da Silva, D. Noriler, and H. F. Meier, "Experiments and CFD-based erosion modeling for gas-solids flow in cyclones," *Powder Technology*, vol. 311, pp. 120-131, 15 April 2017, doi: 10.1016/j.powtec.2016.12.059.
- [27] B. Zhao, Y. Su, and J. Zhang, "Simulation of gas flow pattern and separation efficiency in cyclone with conventional single and spiral double configuration," *Chemical Engineering Research and Design*, vol. 84, no. 12, pp. 1158-1165, December 2006, doi: 10.1205/cherd06040.
- [28] S. G. Bogodage and A. Y. T. Leung, "CFD simulation of cyclone separators to reduce air pollution," *Powder Technology*, vol. 286, pp. 488-506, December 2015, doi: 10.1016/j.powtec.2015.08.023.
- [29] F. Parvaza, S. H. Hosseinib, K. Elsayedc, and G. Ahmadid, "Numerical investigation of effects of inner cone on flow field, performance and erosion rate of cyclone separators," *Separation and Purification Technology*, vol. 201, pp. 223-237, August 2018, doi: 10.1016/j.powtec.2015.08.023.
- [30] I. ANSYS, *ANSYS Fluent Theory Guide*, Technology Drive Canonsburg, PA 15317, November 2013.
- [31] Y. I. Oka, K. Okamura, and T. Yoshida, "Practical estimation of erosion damage caused by solid particle impact. Part 1: effects of impact parameters on predictive equation," *Wear*, vol. 259, no. 1-6, pp. 95-101, July-August 2005, doi: 10.1016/j.wear.2005.01.039.